0026-895X/06/7004-1164–1173$20.00
MOLECULAR PHARMACOLOGY
Copyright © 2006 The American Society for Pharmacology and Experimental Therapeutics
Mol Pharmacol 70:1164–1173, 2006

Vol. 70, No. 4
23820/3135537
Printed in U.S.A.

The Farnesoid X Receptor Promotes Adipocyte Differentiation and Regulates Adipose Cell Function in Vivo

Giovanni Rizzo, Moises Disante, Andrea Mencarelli, Barbara Renga, Antimo Gioiello, Roberto Pellicciari, and Stefano Fiorucci

Dipartimento di Medicina Clinica e Sperimentale, (G.R., M.D., A.M., B.R., S.F.) and Dipartimento di Tecnologia del Farmaco, (A.G., R.P.), University of Perugia, Perugia, Italy

Received February 25, 2006; accepted June 15, 2006

ABSTRACT

The differentiation of a preadipocyte into a mature adipocyte is a highly regulated process that requires a scripted program of transcriptional events leading to changes in gene expression. Several genes are associated with adipogenesis, including the CAAT/enhancer-binding protein (C/EBPs) and peroxisome proliferator-activated receptor (PPAR) families of transcription factors. In this study, we have investigated the role of the farnesoid X receptor (FXR), a bile acid-activated nuclear receptor, in regulating adipogenesis in a preadipocyte cell line (3T3-L1 cells). Our results show that FXR is expressed in the white adipose tissue of adult mice and in differentiated 3T3-L1 cells but not in undifferentiated preadipocytes. Exposure of 3T3-L1 cells to INT-747 (6-ethyl cheno-deoxycholic acid), a potent and selective FXR ligand, increases preadipocyte differentiation induced by a differentiating mixture containing insulin. Augmentation of differentiating mixture-induced differentiation of 3T3-L1 cells by INT-747 associated with induction of aP2, C/EBPα, and PPARγ2 mRNAs along with other adipocyte-related genes. This effect was reversed by guggulsterone, an FXR antagonist, and partially reverted by GW9662 (2-chloro-5-nitro-*N*-phenylbenzamide), a selective PPARγ antagonist, indicating that FXR modulates adipocyte-related genes by PPARγ-dependent and -independent pathways. Regulation of adipocyte-related genes by INT-747 was lost in FXR$-/-$ mice, indicating that modulation of these genes by INT-747 requires an intact FXR. In addition, INT-747 enhances both insulin-induced serine phosphorylation of Akt and glucose uptake by 3T3-L1 cells. Taken together, these results suggest that activation of FXR plays a critical role in regulating adipogenesis and insulin signaling.

The farnesoid X receptor (FXR) is a nuclear receptor and bile acid sensor expressed in liver, intestine, kidney, and adrenal glands (Zhang et al., 2003; Bishop-Bailey et al., 2004). Upon activation, FXR regulates target gene expression by binding to FXR response elements after heterodimerization with the retinoid X receptor (RXR). The optimal DNA binding sequence for the FXR/RXR heterodimer is an inverted repeat of two AGGTCA half-sites spaced by one nucleotide (inverted repeat 1) (Forman et al., 1995).

In target tissues, FXR ligands negatively regulate bile acid synthesis by decreasing the expression of cholesterol-7-hydroxylase (Cyp7a1), the rate-limiting enzyme of the bile acid biosynthetic pathway. This process is partially mediated by induction of the small heterodimer partner (SHP), an atypical nuclear receptor that lacks a DNA binding domain (Goodwin et al., 2000; Lu et al., 2000). FXR controls cholesterol disposal and the enterohepatic circulation of bile acids by increasing the transcription of the intestinal ileal-bile acid binding protein (Grober et al., 1999), inhibiting the hepatic expression/function of the bile acid transporter Na^+-taurocholate cotransporting polypeptide (Denson et al., 2001) and inducing the expression/function of the bile salt export pump (Ananthanarayanan et al., 2001) and multidrug resistance-associated protein 2 (Kast et al., 2002). A growing body of evidence also support the notion that FXR has an important role in regulating lipid (triglyceride and cholesterol) and glucose homeostasis (Sinal et al., 2000; Urizar et al., 2000; Lambert et al., 2003; Claudel et al., 2005). Consistent with this view, FXR gene ablation in mice is associated with increased blood cholesterol and triglyceride levels.

Article, publication date, and citation information can be found at http://molpharm.aspetjournals.org.
doi:10.1124/mol.106.023820.

ABBREVIATIONS: FXR, farnesoid X receptor; RXR, retinoid X receptor; SHP, small heterodimer partner; INT-747, 6-ethyl chenodeoxycholic acid; CDCA, 6-ethyl chenodeoxycholic acid; DMEM, Dulbecco's modified Eagle's medium; FBS, fetal bovine serum; DIM, differentiation mixture; IBMX, 3-iso-butyl-1-methylxanthine; PCR, polymerase chain reaction; qRT-PCR, quantitative real-time PCR; C_T, cycle threshold (the cycle number at which each PCR reaction reaches a predetermined fluorescence threshold); GAPDH, glyceraldehyde-3-phosphate dehydrogenase; C/EBP, CAAT/enhancer-binding protein; PPAR, peroxisome proliferator-activated receptor; FABP, fatty acid binding protein; SREBP-1c, sterol-regulatory element binding protein-1c; TNFα, tumor necrosis factor α; GW9662, 2-chloro-5-nitro-*N*-phenylbenzamide.

Together with the muscle, the adipose tissue is the major regulator of body's energy balance in mammalian (Fruhbeck et al., 2001). Excessive accumulation of adipose tissue leads to obesity, whereas its absence is associated with lipodystrophic syndromes. Adipocytes differentiation is a multistep process where fibroblast-like undifferentiated cells are converted into lipid droplets accumulating cells. Several adipogenic factors are involved in preadipocyte differentiation including members of the CAAT/enhancer binding protein (C/EBP) and peroxisome proliferator-activated receptor (PPAR) families of transcription factors (Lin and Lane, 1994; Tontonoz et al., 1994; Cowherd et al., 1999; Wu et al., 1999). Whether FXR modulates preadipocytes differentiation is still debated.

In this article, we report that FXR is expressed in the adipose tissue and that the synthetic FXR ligand INT-747 [6-ethyl chenodeoxycholic acid (CDCA)] promotes adipocytes differentiation and lipid storage. In addition, we demonstrated that in vivo administration of INT-747 provides a robust induction of FXR target genes in the adipose tissue of wild-type mice but not in FXR−/− mice. Together, these data identify adipocyte-differentiating factors as FXR-regulated genes.

Materials and Methods

Plasmid and Retrovirus 3T3-L1 Infections. Mouse cDNA encoding FXRα and FXR response element reporter plasmid were cloned as in Rizzo et al. (2005). The sequences of the primers used were: gaagctaagg*atg*gtgatgcag and gatgtgcag*tga*tggacaccag. The initiation (atg) and stop (tga) codons are italicized and underlined. FXRα coding sequence was first cloned in pCR2.1 vector (Invitrogen, Carlsbad, CA) and then subcloned in BamHI and XhoI sites into PINCO retroviral vector. Human embryonic kidney 293T modified packaging cell line were cultured in Dulbecco's modified Eagle's medium (DMEM) containing 10% fetal bovine serum (FBS) and transiently transfected with a PINCO-FXR chimera or a PINCO vector alone, as negative control. Forty-eight hours after transfection, the viral supernatant was harvested and used to infect 3T3-L1 cells. The FXR expression was tested by Western blot analysis.

Animals. Homozygous FXR−/− male mice of 12 to 20 weeks of age and sex- and age-matched wild-type control mice (FXR+/+) bred on the C57BL/6j (Sinal et al., 2000) genetic background were housed with a 12-h light/dark cycle with free access to water and standard laboratory chow. Animals were orally administered INT-747 (10 mg/kg/day) for 4 days and sacrificed 4 h after the last dose to collect the abdominal adipose tissue.

Cell Culture, Differentiation Assays, and Glucose Uptake. 3T3-L1 preadipocytes were cultured in DMEM supplemented with 10% FBS, 100 U/ml penicillin, and 100 mg/ml streptomycin in a 5% CO_2 humidified atmosphere and allowed to reach confluence. Differentiation of preadipocytes 2 day after confluence was induced by exposing them to a differentiation mixture (DIM) containing 5 μg/ml insulin, 1 μM dexamethasone, and 0.5 mM 3-iso-butyl-1-methylxanthine (IBMX) in 10% FBS-supplemented DMEM for 48 h (Student et al., 1980). The culture medium was replaced every 48 h with DMEM containing 5 μg/ml insulin. Glucose uptake was measured as described previously (Fiorucci et al., 2004). In brief, fully differentiated adipocytes were starved overnight and then incubated with INT-747 for 18 h at 37°C in glucose uptake buffer (8.1 mM Na_2HPO_4, 1.4 mM KH_2PO_4, 2.6 mM KCl, 136 mM NaCl, 0.5 mM $MgCl_2$, 0.9 mM $CaCl_2$, pH 7.4). 3T3-L1 cells were incubated with 1 μCi of [^{3}H]2-deoxyglucose (PerkinElmer Life and Analytical Sciences, Boston, MA) in glucose uptake buffer for 30 min at room temperature in the presence of 10 nM insulin and 10 nM to 1 μM INT-747. Cells were lysed with ice-cold 1 mM NaOH, and radioactivity was measured using a scintillation counter. Data were expressed in disintegrations per minute per milligram of protein.

Immunoblot Analysis. Total cellular proteins of frozen tissues and cell lines were extracted using a lysis buffer (50 mM HEPES-KOH, pH 7.8, 420 mM KCl, 0,1 mM EDTA, 5 mM MgCl2, 1 mM dithiothreitol, 0.5 mM phenylmethylsulfonyl fluoride, 0,0002% leupeptin, and 20% glycerol), and concentration of proteins were assayed according to the Bradford method. Protein samples were denatured by heating them to 90°C in SDS-reducing buffer and resolved by electrophoresis on 10% SDS-polyacrylamide gels. After protein transfer to the nitrocellulose membranes, the filters were probed with a rabbit polyclonal anti-FXR and β-actin antibodies (Santa Cruz Biotechnology, SantaCruz, CA), anti-Akt, or anti-phospho-Akt (ser473) (Cell Signaling Technology, Danvers, MA). Proteins were then visualized by chemiluminescence using Supersignal Western FEMTO reagent (Pierce, Rockford, IL).

Transactivation Assay. Human embryonic kidney 293T cells were cultured in DMEM. Twenty-four hours before transfection, they were seeded onto six-well plates at a density of 250,000 cells/well. Transient transfections were performed using the calcium phosphate coprecipitation method in the presence of 25 μM chloroquine using 500 ng of pGL3-$(IR1)_3$-Luc reporter vector, 200 ng of pCMV-βgal (internal control for transfection efficiency) and 50 ng of pSG5-FXR and pSG5-RXR. The pGEM vector (Promega, Madison, WI) was added to normalize the amounts of DNA transfected in each assay (2.5 μg). At 36 to 48 h after transfection, cells were stimulated with 20 μM CDCA or 1 μM INT-747 for 18 h, diluted in dimethyl sulfoxide. Control cultures received vehicle (0.1% dimethyl sulfoxide) alone. Cells were lysed in 100 μl of diluted reporter lysis buffer (Promega), and 0.2 μl of cellular lysates was assayed for luciferase activity using the Luciferase Assay System (Promega). Luminescence was measured using an automated luminometer. Luciferase activities were normalized for transfection efficiencies by dividing the relative light units by β-galactosidase activity expressed from cotransfected pCMV-βgal. Each data point was the average of triplicate assays and repeated three times.

qRT-PCR. Quantization of the expression level of selected genes was performed by quantitative real-time PCR (qRT-PCR). Total RNA was isolated with TRIzol reagent (Invitrogen) from 3T3-L1 cells stimulated with FXR ligand for 18 h or from mice tissues. One microgram of RNA was incubated with DNaseI (Invitrogen) for 15 min at room temperature and then at 95°C for 5 min in the presence of 2.5 mM EDTA. The RNA was reverse-transcribed with Superscript III (Invitrogen) with random primers in volume of 20 μl. For real-time PCR, 100 ng of template was used in a 25-μl reaction containing a 0.3 μM concentration of each primer and 12.5 μl of 2× SYBR Green PCR Master Mix (Bio-Rad Laboratories, Hercules, CA). All reactions were performed in triplicate using the following cycling conditions: 2 min at 95°C, followed by 50 cycles of 95°C for 10 s and 60°C for 30 s using an iCycler iQ instrument (Bio-Rad Laboratories). The mean value of the replicates for each sample was calculated and expressed as cycle threshold (C_T), the cycle number at which each PCR reaction reaches a predetermined fluorescence threshold, set within the linear range of all reactions. The amount of gene expression was then calculated as the difference (ΔC_T) between the C_T value of the sample for the target gene and the mean C_T value of that sample for the endogenous control (GAPDH). Relative expression was calculated as the difference ($\Delta\Delta C_T$) between the ΔC_T values of the test and control samples for each target gene. The relative level of expression was measured as $2^{-\Delta\Delta C_T}$. All PCR primers were designed using the software PRIMER3-OUTPUT using published sequence data obtained from the NCBI database. Mouse primers were as follows: FXR-α, tgggctccgaatcctcttaga and tggtcctcaaataagatcctgg; PPARγ2, gccagtttcgatccgtagaa and aatccttggccctctgagat; SREBP1c, gatcaaagaggagccagtgc and tagatggtggctgctgagtg; SHP, tctcttcttccgccctatca and aagggcttgctggacagtta; ADIPOQ, cagtggatctgacgacaccaa and gaacaggagagcttgcaacagt; aP2, agtgaaaacttcgatgat-

tacatgaa and gcctgccactttccttgtg; C/EBPα, gacatcagcgcctacatcga and tcggctgtgctggaagag; TNF-α: acggcatggatctcaaagac and gtgggtgagcacgtagt; GAPDH, ctgagtatgtcgtggagtctac and gttggtggtgcaggatgcattg.

Oil Red O Staining and Immunohistochemistry. Dishes were washed in PBS, and cells were fixed in 3.7% formaldehyde for 1 h, followed by staining with Oil Red O for 1 h. Oil Red O was prepared by diluting a stock solution [0.5 g of Oil Red O (Sigma) in 100 ml of isopropanol] with water (6:4) followed by filtration. After staining, plates were washed twice in water and photographed. For immunohistochemistry, 500,000 cells were spread on poly-L-lysine–coated slides (150 μl/slide) by using a cytospin. The slides were subsequently fixed in ethanol/acetone [1:1 (v/v)] for 10 min at −20°C and incubated for 30 min at 94–98°C in buffer (0.1 M sodium citrate and 0.1 M citric acid, pH 6). After a wash in Tris-buffered saline/Tween 20 (3 g/l Trizma base, 8 g/l NaCl, 0.2 g/l KCl, and 0.05% Tween 20, pH 8) containing 10% rabbit serum, slides were incubated with a polyclonal anti-FXR antibody (Santa Cruz Biotechnology) for 30 min at room temperature. The secondary antibody and revelation methods were from Histostain-*Plus* Kit (Zymed, South San Francisco, CA).

Statistical Analysis. Data are expressed as mean ± S.E. The analysis of variance with Bonferroni correction for multiple comparisons (Prism 3; GraphPad Software. Inc., San Diego, CA) was used to assess significant statistical difference between groups.

Results

FXR Was Expressed on Adipose Tissue and Adipocyte Cell Line. We first investigated whether FXR was expressed by adipocytes and white adipose tissue. Results from these experiments, shown in Fig. 1A, demonstrated FXR protein expression in the white adipose tissue obtained from adult (12 weeks old) C57BL/6j mice but not in undifferentiated 3T3-L1 cells, a preadipocyte cell line. Confirming these findings, FXR-like immunoreactivities with a nuclear localization were detected in terminally differentiated 3T3-L1 cells but not in preadipocytes (Fig. 1, B versus D). The expression of the FXR mRNA was robustly induced during in vitro differentiation of 3T3-L1 cells (8-day culture with DIM) (Fig. 1E); a significant induction of FXR mRNA expression was detected at day 2 (≈2-fold increase over the baseline) and peaked at day 4 (≈4-fold increase over the baseline; $p < 0.05$ versus day 0). In addition, adipocyte differentiation was associated with increased expression of SHP (Fig. 1F), a known FXR-regulated gene ($p < 0.05$ versus day 0). A similar pattern of gene expression was observed in 3T3-L1 cells exposed to 10 μM CDCA, a naturally occurring FXR ligand (data not shown).

Activation of FXR Enhanced Differentiation of a Preadipocyte Cell Line. Differentiation of 3T3-L1 cells into mature adipocytes was evaluated by assessing the accumulation of triacylglycerol in Oil Red O-stained vesicles and expression of adipocyte-related genes. As illustrated in Fig. 2A, 8-day exposure to a combination of DIM and a semisynthetic FXR ligand, INT-747 (1 μM), resulted in a robust induction of cell differentiation compared with DIM alone. 3T3-L1 cells treated with INT-747 in combination with DIM show larger lipid droplets and stronger staining with Oil Red O than cells treated with DIM alone (Fig. 2, D versus C). INT-747 alone failed to induce differentiation of 3T3-L1 cells (Fig. 2E). A number of adipocyte-related genes were induced

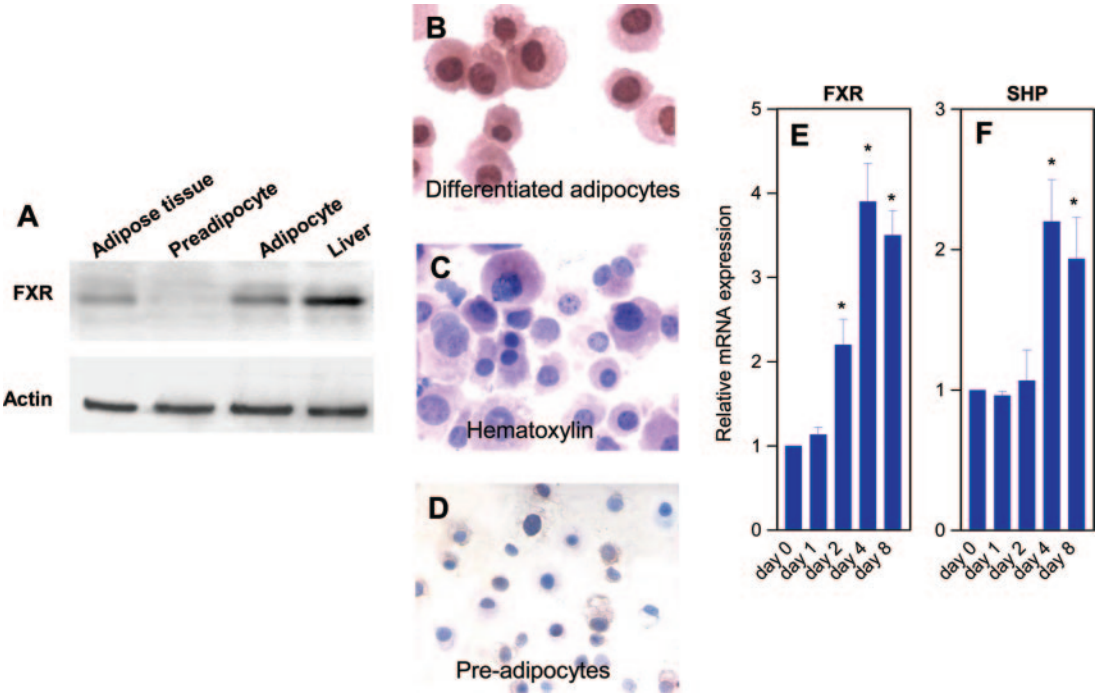

Fig. 1. Preadipocyte differentiation associated with induction of FXR gene expression. A, Western blot analysis showing FXR protein expression by white abdominal adipose tissue and differentiated 3T3-L1 cells (adipocytes). Two days after confluence, 3T3-L1 preadipocytes were induced to differentiate with DIM (a cocktail of 5 μg/ml insulin, 1 μM dexamethasone, and 0.5 mM IBMX) and maintained in culture for 8 days as described under *Materials and Methods*. Liver lysates were used as a control. The blot shown is representative of three others showing the same pattern. B–D, immunohistochemistry analysis of FXR expression by differentiated and nondifferentiated 3T3-L1 cells. Magnification, 40×. B, nuclear localization of FXR-like immunoreactivity in terminally differentiated 3T3-L1 cells. C, hematoxylin counterstaining of mature 3T3-L1 cells showing no background in control slides prepared by omitting the secondary antibody. D, preadipocytes lack FXR expression. FXR-immunostaining and hematoxylin counterstaining. E and F, qRT-PCR analysis of FXR and SHP expression in 3T3 cells. Values are normalized relative to GAPDH and expressed as means ± S.E.M. relative to day 0, which is arbitrarily set as 1. Data shown are mean ± S.E. of six experiments. *, $p < 0.05$ versus day 0.

by FXR activation. Exposure of DIM-treated 3T3-L1 cells to INT-747 enhanced the expression of C/EBPα, PPARγ2 (Tontonoz et al., 1994; Fu et al., 2005; Li et al., 2005); fatty acid binding protein (FABP), also called aP2 (Christy et al., 1989); adipocyte determination and differentiation factor-1/sterol-regulatory element binding protein-1c (ADD1/SREBP-1c) (Kim and Spiegelman, 1996); adipoQ, and adiponectin (Yamauchi et al., 2003) (Fig. 2, F–J; $n = 6$; $p < 0.05$ versus DIM alone). In addition, INT-747 corroborated the DIM-induced down-regulation of TNF-α mRNA (Xu and Hotamisligil, 2001) (Fig. 2K; $n = 6$; $p < 0.05$ versus DIM alone). Similar results were obtained by exposing the cells to CDCA (20 μM) (Fig. 2, F–K, $p < 0.05$ versus DIM alone). In contrast to the ability of FXR ligands to potentiate the DIM-induced differentiation of adipocytes, both the natural and synthetic FXR ligands failed to induce 3T3-L1 differentiation when tested alone (Fig. 2, F–K). Thus, FXR activation enhances DIM-induced adipogenesis and regulates genes involved in adipocyte differentiation/function.

FXR Antagonism Prevents Preadipocyte Differentiation Induced by INT-747. To investigate whether augmentation of DIM-induced differentiation by INT-747 was mediated by FXR activation, INT-T47 treated 3T3-L1 cells were exposed to guggulsterone, a known FXR antagonist (Urizar et al., 2002). Results shown in Fig. 3A demonstrate that guggulsterone antagonizes the effect of INT-747 and CDCA on FXR transactivation ($p < 0.05$ versus CDCA- or INT-747-treated cells). In addition (Fig. 3B), exposure to guggulsterone (10 μM) resulted in a dramatic reduction of 3T3-L1 cell size and lipid droplet accumulation (Fig. 3, D versus C). Furthermore, the expression of all INT-747-regulated genes was inhibited by guggulsterone (Fig. 3E; $n = 5$; $p < 0.05$ versus cells treated with INT-747). Guggulsterone alone had no effect on gene expression except in TNF-α, which it weakly inhibited (Shishodia and Aggarwal, 2004).

Retroviral Expression of FXR Enhanced DIM-Induced Differentiation. We then investigated whether ectopic overexpression of FXR enhanced DIM-induced differentiation of preadipocytes. For this purpose, FXR overexpressing 3T3-L1 cells were induced to differentiate with DIM in combination with INT-747. 3T3-L1 cells infected with the vector alone were used as a control. As shown in Fig. 4, A and

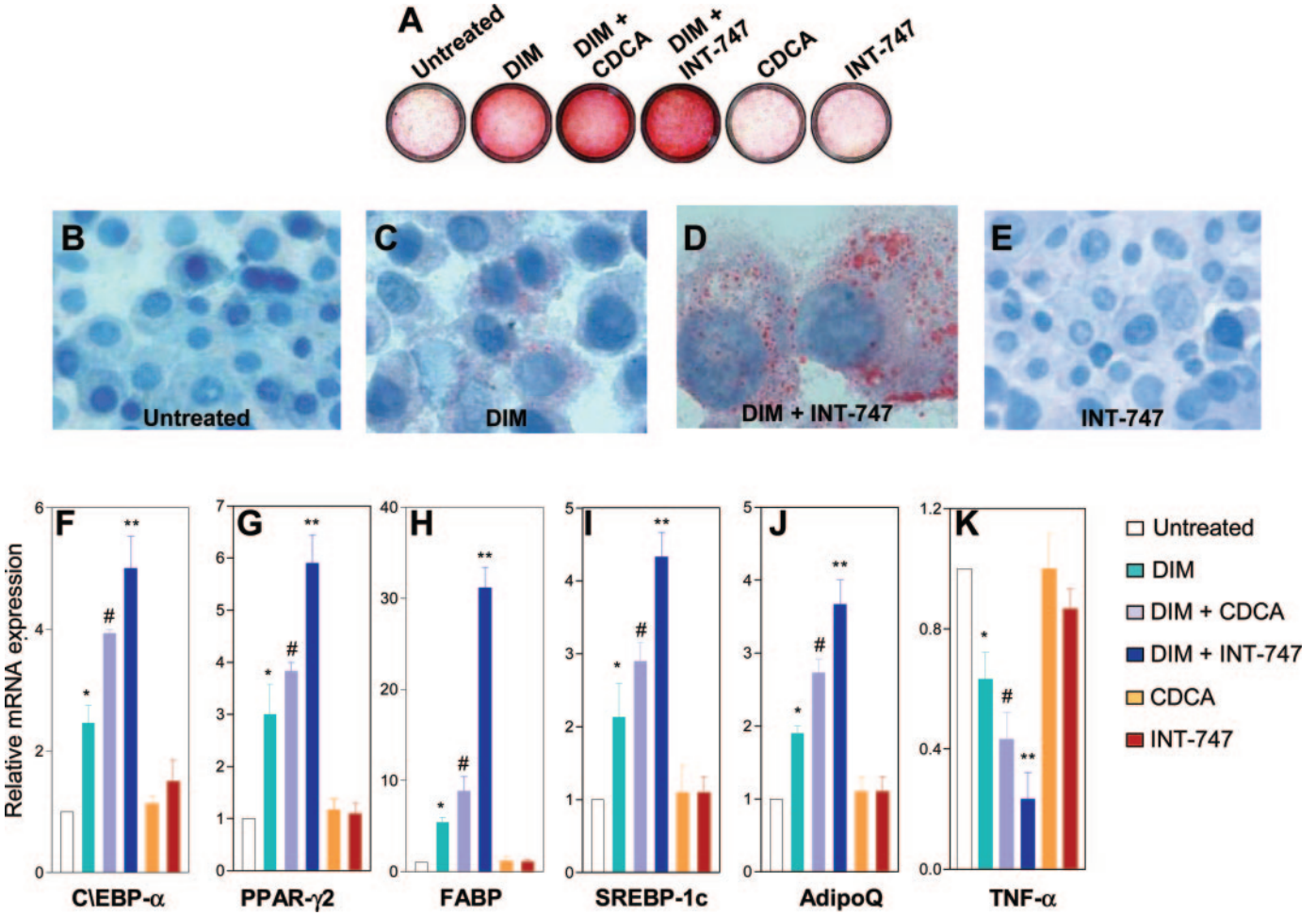

Fig. 2. FXR activation enhanced DIM-induced adipogenesis in 3T3-L1 preadipocytes. A, Oil Red O staining of triacylglycerol-containing vesicles in 8-day culture 3T3-L1 cells. CDCA and INT-747 enhanced the DIM-induced differentiation. B–E, day-8 cultures of 3T3-L1 cells were exposed to INT-747 alone or in combination with DIM. Cytospins were then stained with Oil Red O. Cells exposed to INT-747 alone showed a larger cytoplasm and larger lipid droplets than cells treated with DIM alone (D versus C). Exposure to INT-747 alone, however, failed to induce differentiation (E). Magnification, 100×. F–K, regulation of adipocyte-related genes by FXR ligands CDCA and INT-747. Exposure to CDCA (20 μM) and INT-747 (1 μM) in combination with DIM caused a significant induction of C/EBPα, FABP, PPARγ2, SREBP-1c, and AdipoQ expression and ~2-fold reduction of TNF-α. CDCA and INT-747 alone failed to modulate gene expression. *, $p < 0.05$ versus untreated cells; #, $P < 0.05$ CDCA versus DIM alone; **, $p < 0.01$ INT-747 versus DIM alone. Values are normalized to GAPDH and are expressed as means ± S.E.M. of six experiments.

B, at day 4, FXR-overexpressing cells were almost totally differentiated. This phenotype correlates with a robust induction of adipocyte-related genes as measured by qRT-PCR (Fig. 4C; $n = 6$, $p < 0.05$ versus vector alone).

INT-747 Induced Expression of Genes of Lipid Storage and Differentiation in Vivo. We then investigated whether the effect elicited by INT-747 on adipose cells was maintained in vivo. For this purpose, naive C57BL/6j mice and FXR−/− mice (Sinal et al., 2000) were orally administered INT-747 (10 mg/kg/day) for 4 days, and adipose tissue expression of genes involved in adipocyte differentiation and lipid storage was assessed by qRT-PCR. As shown in Fig. 5, in vivo FXR activation induces the expression of FABP, C/EBP-α, PPARγ2, and SREBP-1c and reduced TNF-α mRNA expression in the abdominal fat of wild-type mice (Fig. 5; $p < 0.05$ versus wild-type naive mice). In contrast, INT-747 failed to modulate the expression of C/EBP-α, PPARγ2, and SREBP-1c in FXR−/− mice (Fig. 5; $p < 0.05$ versus naive wild-type mice). Although the expression of FABP was significantly induced by INT-747 in FXR+/+ mice (Fig. 5; $p < 0.05$ versus wild-type naive mice) it was still up-regulated by INT-747 in FXR−/− mice (Fig. 5; $p < 0.05$ versus naive FXR−/− mice). Likewise, we observed that INT-747 weakly down-regulated TNF-α mRNA expression in FXR−/− mice (Fig. 5; $p < 0.05$ versus naive FXR−/−).

INT-747 Induces Differentiation by PPAR-Dependent and -Independent Pathways. It has been shown in loss-of-function studies that PPARγ2 is required for in vivo and in vitro adipogenesis (Wu et al., 1995). Because INT-747 up-regulates the expression of PPARγ2 in the adipose tissue and in 3T3-L1 cells (Fig. 2G), we then investigated whether the INT-747-enhanced DIM-induced differentiation would depend on PPARγ2. For this purpose, 3T3-L1 preadipocytes were induced to differentiate by treatment with DIM and INT-747 in the presence or absence of GW9662 (1 μM), a selective PPARγ antagonist. Treatment with the GW9662 partially reversed the effect of INT-747 on cell differentiation

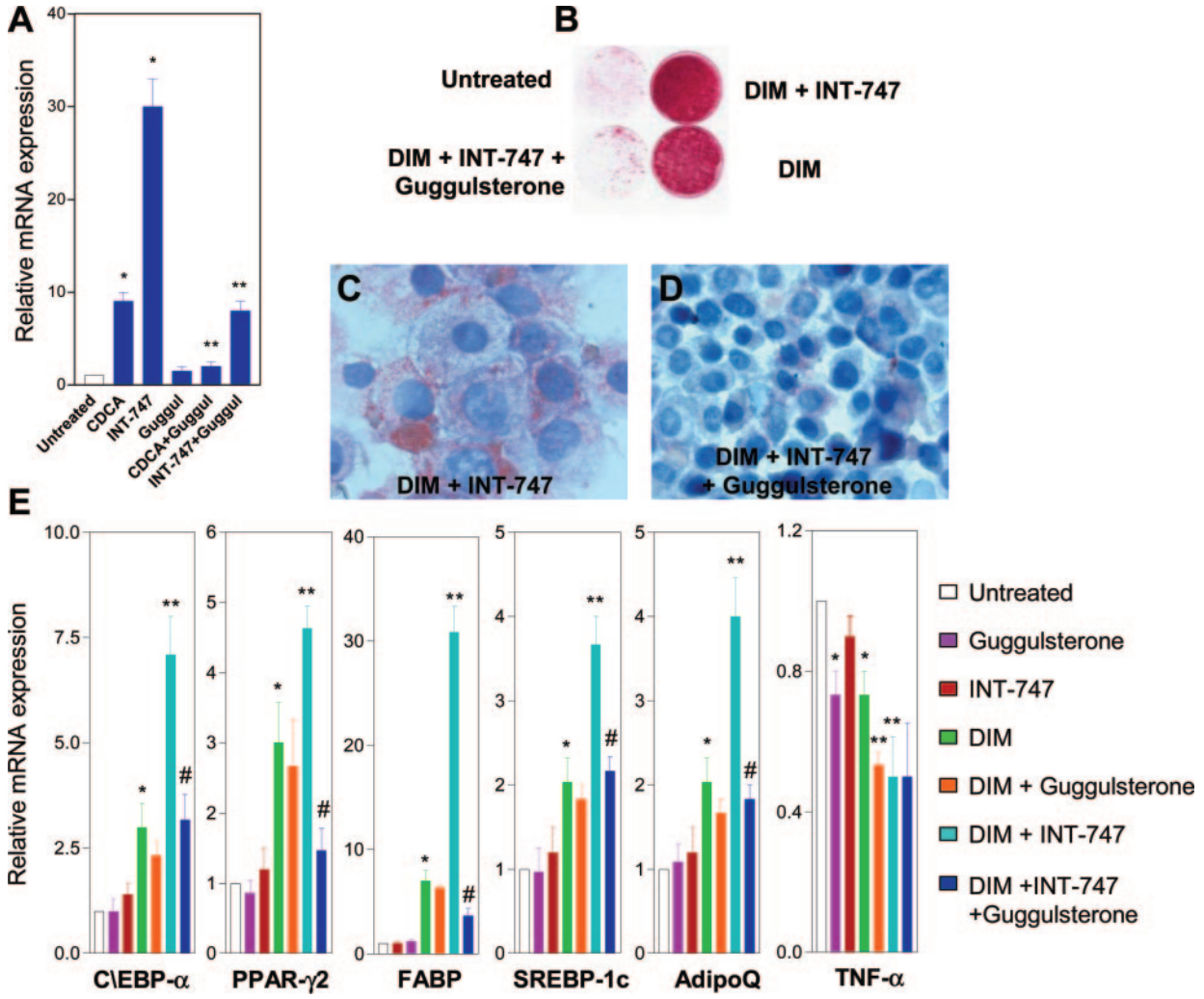

Fig. 3. FXR antagonism prevented preadipocyte differentiation induced by INT-747. 3T3-L1 preadipocytes were induced to differentiate by treatment with DIM in combination with INT-747, in the presence or absence of 10 μM guggulsterone for 8 days. A, guggulsterone antagonized the effect of INT-747 and CDCA on FXR transactivation. Data shown are means ± S.E.M. of four experiments. *, $P < 0.05$ versus untreated; **, $p < 0.05$ versus FXR ligands. B, Oil Red O staining of 3T3-L1 cells in a 8-day culture. Treatment with guggulsterone almost completely abrogates INT-747-induced adipogenesis. C and D, Oil Red O staining of 3T3-L1 cytospins (8-day culture). Magnification, 40×. Guggulsterone-treated 3T3-L1 cells showed reduced size and lipid droplet accumulation in the cytoplasm compared with cells treated with INT-747 alone. E, guggulsterone antagonized the transcriptional effects of INT-747 on FXR-regulated genes. Values are normalized to GAPDH and expressed as means ± S.E.M. of five experiments. *, $p < 0.05$ versus untreated cells; **, $p < 0.05$ versus cells treated with DIM; #, $p < 0.05$ versus cells treated with DIM plus INT-747.

(Fig. 6A) as measured by Oil Red O staining (Fig. 6, C versus B). In addition, exposure to GW9662 antagonized the transcriptional effects of the FXR ligand on FABP, PPARγ2, and SREBP-1c (Fig. 6D; $n = 4$; $p < 0.05$ versus cells treated with INT-747), whereas it had no effect on FXR-mediated modulation of C/EBP-α, TNF-α, and AdipoQ gene expression (Fig. 6D).

INT-747 Causes Akt Phosphorylation and Glucose Uptake. Because INT-747 enhanced DIM-induced preadipo-

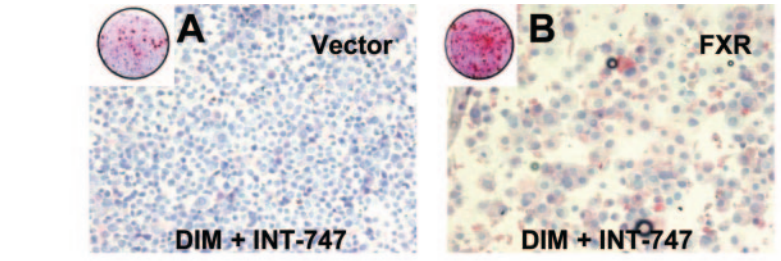

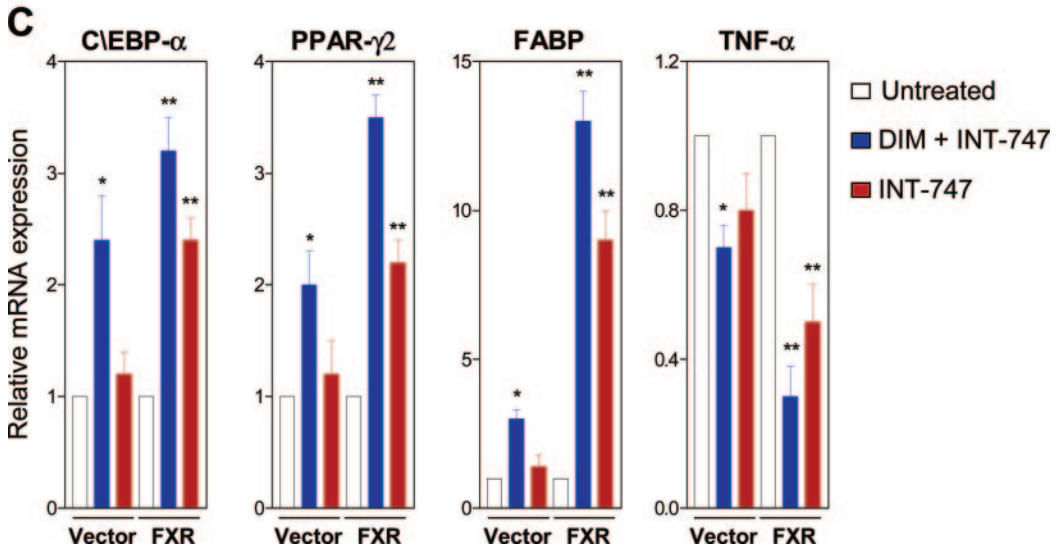

Fig. 4. Forced expression of FXR enhances DIM-induced differentiation of 3T3-L1 cells. A and B, Oil Red O stained 3T3-L1 cells in a 4-day culture. FXR overexpressing cells were already partially differentiated in contrast to cells infected with the vector alone. Magnification, 10×. Inset, Oil Red O staining of 3T3-L1 plates in a 4-day culture. C, qRT-PCR analysis of FXR regulated genes. *, $p < 0.05$ versus untreated cells; **, $p < 0.05$ versus cells transfected with the vector alone. Values are normalized to GAPDH and are expressed as means ± S.E.M. of six experiments.

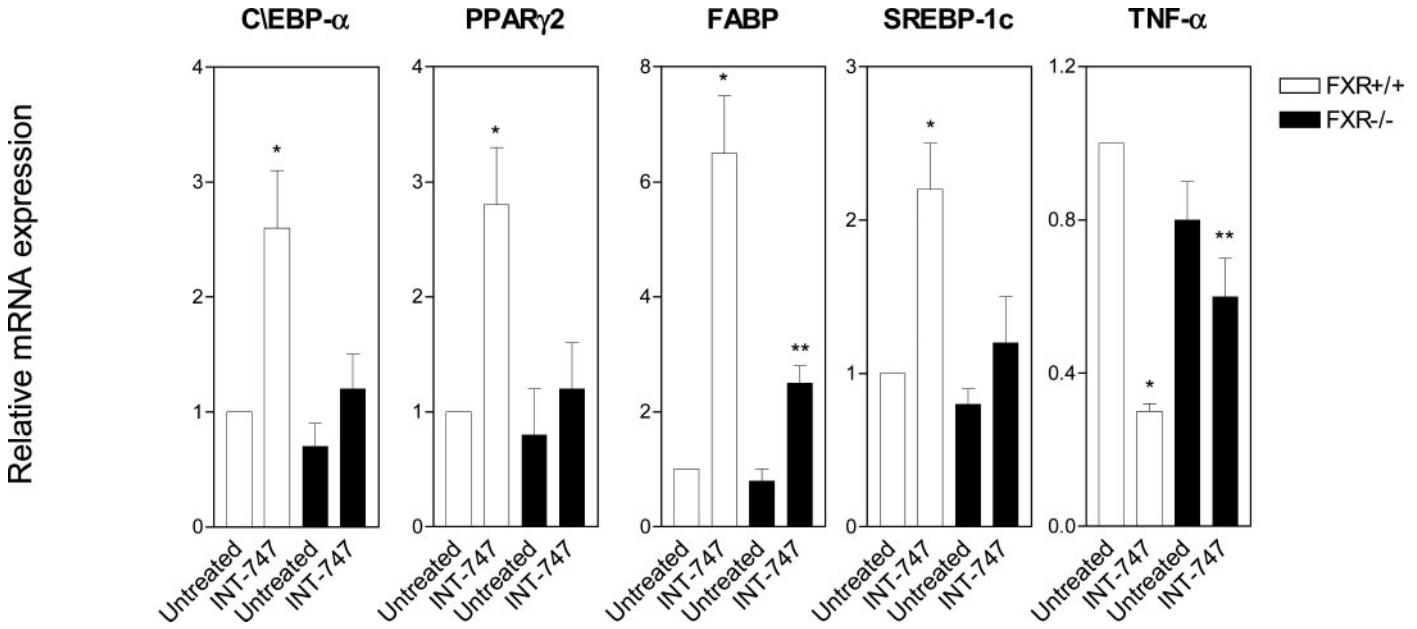

Fig. 5. In vivo FXR activation induced expression of genes involved in lipid storage and adipocyte differentiation. FXR wild-type on C57BL/6j background and FXR−/− mice were administered with INT-747 (10 mg/kg/day) orally for 4 days and the expression of genes involved in adipocyte differentiation and lipid storage in the abdominal adipose tissue assessed by qRT-PCR. Values are expressed as means ± S.E.M. of four to six mice. *, $p < 0.05$ versus wild-type naive mice; **, $p < 0.05$ versus FXR−/− naive mice.

cyte differentiation, we then investigated whether FXR activation enhanced serine 473 phosphorylation of Akt/PKB in 3T3-L1 cells. As shown in Fig. 7, INT-747 produces a robust induction of serine Akt phosphorylation (Fig. 7A), resulting in 3.4 ± 0.6-fold induction of Akt phosphorylation compared with insulin alone as assessed by densitometric analysis (n = 3). In addition, INT-747 significantly enhanced glucose uptake induced by insulin in a dose-dependent manner (Fig. 7B). Taken together, these results indicate that FXR activation might improve insulin signaling in adipocytes.

Discussion

In the present study, we have shown that activation of FXR by natural and synthetic ligands regulates adipocyte differentiation and function. There is an increasing awareness that cross-talk does exist between nuclear receptors that regulate lipid (cholesterol and triglycerides), bile acid metabolism, glucose utilization, and energy balance. Indeed, phenotype-based epidemiologic studies have shown a positive correlation between elevated levels of triglycerides and the incidence of gallbladder stones, a gallbladder-related pathology that is highly prevalent in the metabolic syndrome and in patients with type 2 diabetes. Furthermore, treatment of gallstone patients with bile acids is associated with reduction of plasma triglycerides (Watanabe et al., 2004). This phenotype-based evidence has led to the notion that in genotype-sensible backgrounds, the interaction of nutrients and metabolic intermediates with nuclear receptors may contribute to the development of the typical features of the metabolic syndrome (obesity, insulin resistance, and vascular inflammation), a highly prevalent disease in Western countries.

Together with muscle, the adipose tissue is the major regulator of energy balance in mammalians (Fruhbeck et al., 2001). Excessive accumulation of adipose tissue leads to obesity, whereas its absence is associated with lipodystrophic syndromes. Although FXR is not expressed in skeletal muscles (Huber et al., 2002), its expression has been detected in the adipose tissue (Zhang et al., 2003; Li et al., 2005). We now provide evidence that FXR is expressed by differentiating adipocytes at both the mRNA and the protein levels (Cariou et al., 2006). In addition, by immunohistochemistry analysis, we have shown that FXR retains a nuclear localization.

In this study, we have focused on 3T3-L1 cell differentia-

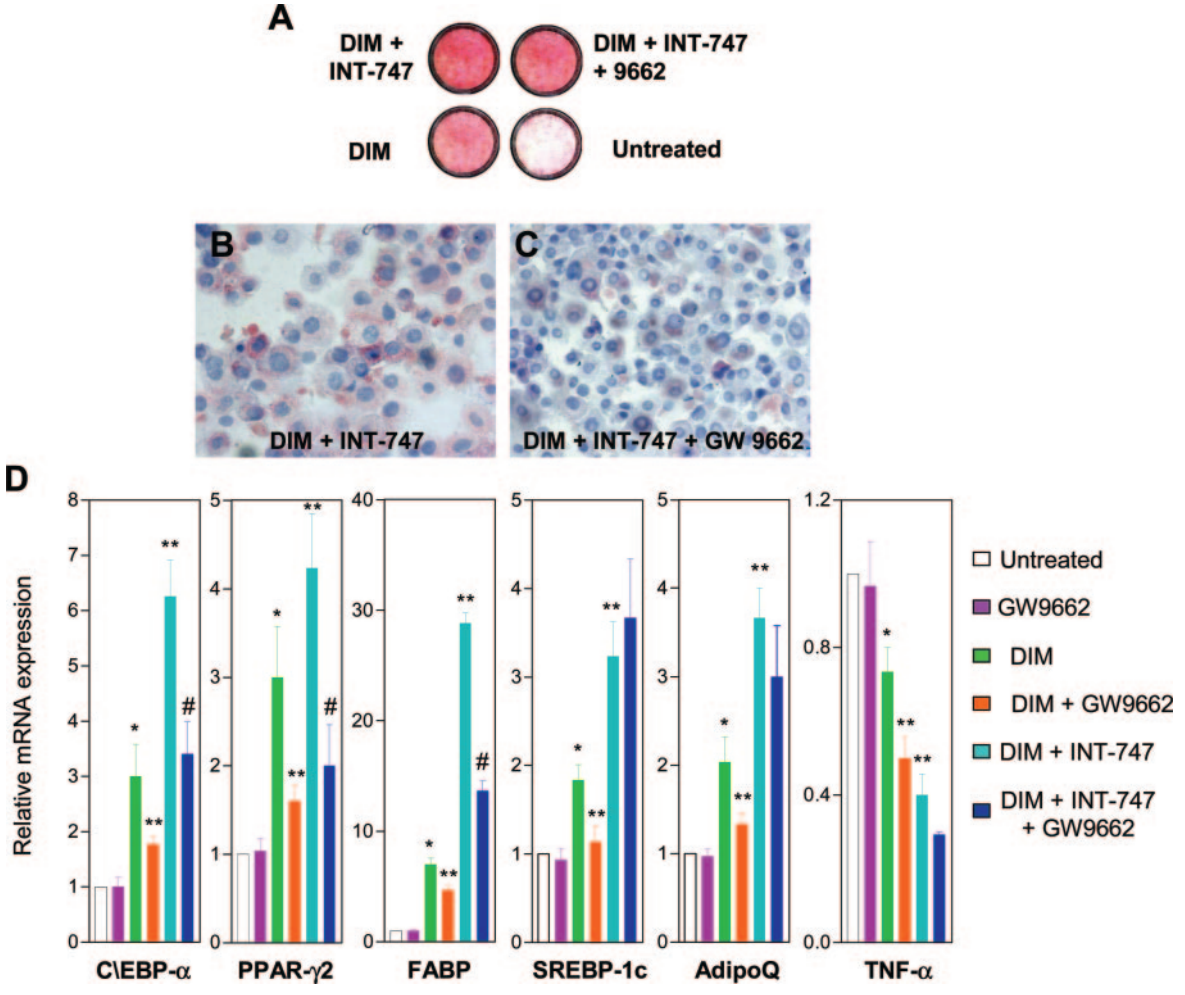

Fig. 6. INT-747 induced differentiation of 3T3-L1 cells by PPAR-dependent and -independent mechanisms. 3T3-L1 preadipocytes were cultured as in Fig. 2 and induced to differentiate by treatment with DIM and INT-747 in the presence or absence of the PPARγ antagonist GW9662 (1 μM). A, Oil Red O staining of 3T3-L1 cells in a 8-day culture. B and C, Oil Red O staining of 3T3-L1 cells. GW9662 antagonized the effect of INT-747. Magnification, 10×. D, GW9662 antagonized the transcriptional effects of INT-747 on C/EBP-α, PPARγ2, FABP and SREBP-1c. Values are normalized to GAPDH and expressed as means ± S.E.M. of four experiments. *, $p < 0.05$ versus untreated cells; **, $p < 0.05$ versus cells treated with DIM alone; #, $p < 0.05$ versus cells treated with DIM plus INT-747.

tion into adipocytes, a well-characterized model of adipogenesis. Analysis of FXR gene expression during adipogenesis in this cell line demonstrates that FXR mRNA is rapidly induced in response to DIM (a hormone cocktail of insulin, dexamethasone, and IBMX). Thus, although FXR was undetectable in undifferentiated adipocytes, its expression became detectable after 2 days in culture and peaked after 4 days of exposure to the inducing mixture. Activation of FXR by INT-747 in this experimental setting resulted in a rapid acquisition of an adipocyte-like phenotype, and cells exposed to INT-747 demonstrated larger lipid droplets and cytoplasm than cells treated with DIM alone. In addition, exposure to natural and synthetic FXR ligands enhanced the expression of a number of DIM-regulated adipocyte-related genes, including C/EBPα, PPARγ2, FABP, and SREBP-1c, and down-regulated the expression of TNF-α, a key mediator of lipolysis.

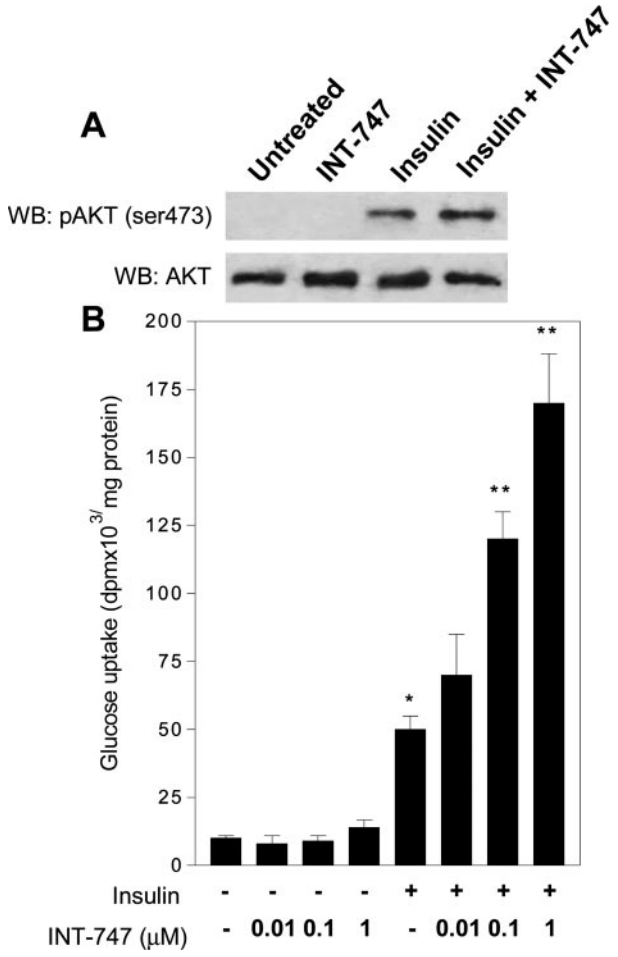

Fig. 7. FXR activation induced serine Akt phosphorylation in 3T3-L1 cells. 3T3-L1 were induced to differentiate for 8 days, treated with INT-747 (1 μM) for 4 h and then exposed to insulin for 5 min. Cell lysates were Western blotted using an anti-phospho-Akt (serine 473) or an anti-Akt antibody that recognizes its phosphorylated and unphosphorylated forms (total). A, exposure to INT-747 in combination with insulin induced serine phosphorylation of Akt (top). The levels of Akt protein were unchanged by the treatment with INT-747 or insulin as shown by Western blot analysis of total Akt expression (bottom). The blot shown is representative of three others showing the same pattern. Exposure to INT-747 caused a 3.4 $\pm$ 0.6-fold increase of phosphorylated Akt in comparison with DIM alone as quantified by densitometric analysis (n = 3). B, INT-747 enhanced insulin-stimulated glucose uptake in 3T3-L1 adipocytes. Cells were incubated with the indicated concentrations of INT-747 for 18 h and then stimulated with insulin (10 nM) for 30 min. Data are expressed as means $\pm$ S.E.M. of three independent experiments. *, $p < 0.05$ versus untreated cells and **, $p < 0.05$ versus cells treated with insulin alone.

In this study, we showed that augmentation of DIM-induced differentiation by INT-747 was almost completely abrogated by guggulsterone. Guggulsterone, the active ingredient of the resin of the guggul tree (*Commiphora mukul*), has been used to treat a variety of ailments, including obesity and lipid disorders (Urizar and Moore, 2003). In transient transfection assay of mouse hepatocytes with a synthetic FXR responsive reporter plasmid, (*Z*)-guggulsterone, one of the two active isomers of guggulsterone, alone had no effect on FXR activity, but it strongly inhibited (≈90%) FXR activation induced by CDCA (Urizar et al., 2002). Although it acts as an FXR antagonist in the coactivator association assay, guggulsterone enhances FXR-induced transcription of bile salt exporting pump, a major hepatic bile acid transporter and FXR target in HepG2 cells (Cui et al., 2003). In this study, we showed that guggulsterone inhibits INT-747-induced FXR transactivation in a gene reporter assay and that it antagonizes the pro-differentiating activity of INT-747 on adipocytes. This effect might negatively affect the lipid-lowering effect of guggulsterone and might therefore contribute to explain the lack of positive results observed in clinical settings with this agent (Urizar et al., 2002; Urizar and Moore, 2003). In addition to its anti-FXR activities, there is evidence that guggulsterone is a promiscuous ligand for several steroid hormone receptors including the glucocorticoid and mineralocorticoid receptors and the androgen receptor (Burris et al., 2005). Previous studies have shown that ligands for glucocorticoids might induce adipogenesis (MacDougald and Mandrup, 2002). However, it is unlikely that such a mechanism explains the counter-regulatory effect of guggulsterone in this experimental setting, taking into account that INT-747 has no activity on the glucocorticoid receptor (Pellicciari et al., 2002). In addition, guggulsterone does not interact with PPARs, RXRs, thyroid receptor, and liver X receptors (Burris et al., 2005).

The critical role of FXR in regulating adipocyte differentiation was further examined in transfection studies. Indeed, we observed that overexpression of FXR in 3T3-L1 results in augmentation of DIM-induced cell differentiation. Moreover, the adipocyte-relative genes were robustly induced by FXR overexpression in these experimental settings.

In vivo experiments on chow-fed wild-type and FXR−/− mice have shown that activation of FXR with INT-747 enhances the expression of C/EBP-α, PPARγ2, and FABP in the adipose tissue while inhibiting the expression of TNF-α in wild-type mice, suggesting that FXR is involved in regulating either adipogenesis, by inducing C/EBPα and PPARγ2 genes, or lipid storage, by inducing FABP and inhibiting TNF-α. INT-747 also induces SREBP-1c mRNA expression in the white adipose tissue (Rosen et al., 2000), providing evidence for a regulatory role of FXR expression/function of SREBP-1c in adipocyte. Because these effects were not observed in FXR−/− mice, it seems that INT-747 administration requires an intact FXR gene to elicit its metabolic activities. Furthermore, it has previously been demonstrated that murine embryonic fibroblasts isolated from FXR−/− mice were unable to correctly accumulate triglyceride during the course of differentiation (Cariou et al., 2006).

Previous studies have shown that FXR induces PPARγ2 in vitro and in vivo. Because PPARγ2 is a key regulatory factor

for adipocyte differentiation, we have investigated whether FXR regulates adipogenesis in a PPARγ2-dependent manner. However, results obtained with GW9662, a PPARγ antagonist, suggest that only part of the transcriptional effects induced by INT-747 were mediated by PPARγ. Thus, FXR regulates adipogenesis by a PPARγ-dependent and -independent mechanism.

A growing body of evidence indicates that FXR might regulate insulin signals in adipocytes. Support for this concept comes from the observation that FXR deficiency alters the level of phosphorylation of Akt/PKB in the white adipose tissue, and to a lesser extent in skeletal muscles (Cariou et al., 2006), and that GW4064, a nonsteroidal FXR ligand, increases the level of serine 473 phosphorylation of Akt/PKB and glucose uptake in 3T3-L1 adipocytes exposed to insulin (Cariou et al., 2006). We have now shown that INT-747 increases Akt/PKB phosphorylation and glucose uptake in insulin-primed 3T3-L1 cells, suggesting that these activities might contribute to the pro-differentiating activity of INT-747 in this cell line.

Consistent with the role of FXR in regulating the adipocyte function, FXR−/− mice have a decreased fat mass with a reduced adipocyte size (Cariou et al., 2006). In addition, FXR−/− mice exhibit increased levels of circulating FFA that may contribute to their peripheral insulin resistance. It has also been shown that FXR activation increases glucose uptake in adipocytes and improves insulin sensitivity in vivo in *ob/ob* mice, a mouse model of insulin resistance (Cariou et al., 2006). In conjunction with present results, FXR activation seems to lead to reduced synthesis of fatty acid in the liver and increased lipid storage in the adipose tissue. The net physiological effect of these two coordinated activities would be a reduction of circulating triglycerides, an effect that is observed in rodents exposed to FXR ligands (Zhang et al., 2006).

In summary, we have shown that FXR was expressed in the adipose tissue and that the synthetic FXR ligand INT-747 promoted adipocyte differentiation, adipogenesis, and lipid storage in vivo and in vitro. Together, our results identify adipocyte-differentiating factors as FXR-regulated genes and support the notion that FXR ligands might have utility in the treatment of metabolic disorders.

References

Ananthanarayanan M, Balasubramanian N, Makishima M, Mangelsdorf DJ, and Suchy FJ (2001) Human bile salt export pump promoter is transactivated by the farnesoid X receptor/bile acid receptor. *J Biol Chem* **276:**28857–28865.

Bishop-Bailey D, Walsh DT, and Warner TD (2004) Expression and activation of the farnesoid X receptor in the vasculature. *Proc Natl Acad Sci USA* **101:**3668–3673.

Burris TP, Montrose C, Houck KA, Osborne HE, Bocchinfuso WP, Yaden BC, Cheng CC, Zink RW, Barr RJ, Hepler CD, et al. (2005) The hypolipidemic natural product guggulsterone is a promiscuous steroid receptor ligand. *Mol Pharmacol* **67:**948–954.

Cariou B, van Harmelen K, Duran-Sandoval D, van Dijk TH, Grefhorst A, Abdelkarim M, Caron S, Torpier G, Fruchart JC, Gonzalez FJ, et al. (2006) The farnesoid X receptor modulates adiposity and peripheral insulin sensitivity in mice. *J Biol Chem* **281:**11039–11049.

Christy RJ, Yang VW, Ntambi JM, Geiman DE, Landschulz WH, Friedman AD, Nakabeppu Y, Kelly TJ, and Lane MD (1989) Differentiation-induced gene expression in 3T3–L1 preadipocytes: CCAAT/enhancer binding protein interacts with and activates the promoters of two adipocyte-specific genes. *Genes Dev* **3:**1323–1335.

Claudel T, Staels B, and Kuipers F (2005) The farnesoid X receptor: a molecular link between bile acid and lipid and glucose metabolism. *Arterioscler Thromb Vasc Biol* **25:**2020–2030.

Cowherd RM, Lyle RE, and McGehee RE Jr (1999) Molecular regulation of adipocyte differentiation. *Semin Cell Dev Biol* **10:**3–10.

Cui J, Huang L, Zhao A, Lew JL, Yu J, Sahoo S, Meinke PT, Royo I, Pelaez F, and Wright SD (2003) Guggulsterone is a farnesoid X receptor antagonist in coactivator association assays but acts to enhance transcription of bile salt export pump. *J Biol Chem* **278:**10214–10220.

Denson LA, Sturm E, Echevarria W, Zimmerman TL, Makishima M, Mangelsdorf DJ, and Karpen SJ (2001) The orphan nuclear receptor, shp, mediates bile acid-induced inhibition of the rat bile acid transporter, ntcp. *Gastroenterology* **121:**140–147.

Fiorucci S, Mencarelli A, Distrutti E, Baldoni M, del Soldato P, and Morelli A (2004) Nitric oxide regulates immune cell bioenergetic: a mechanism to understand immunomodulatory functions of nitric oxide-releasing anti-inflammatory drugs. *J Immunol* **173:**874–882.

Forman B, Goode E, Chen J, Oro AE, Bradley DJ, Perlmann T, Noonan DJ, Burka LT, McMorris T, Lamph WW, et al. (1995) Identification of a nuclear receptor that is activated by farnesol metabolites. *Cell* **81:**687–693.

Fruhbeck G, Gomez-Ambrosi J, Muruzabal FJ, and Burrell MA (2001) The adipocyte: a model for integration of endocrine and metabolic signaling in energy metabolism regulation. *Am J Physiol* **280:**E827–E847.

Fu M, Sun T, Bookout AL, Downes M, Yu RT, Evans RM, and Mangelsdorf DJ (2005) A nuclear receptor atlas: 3T3–L1 adipogenesis. *Mol Endocrinol* **19:**2437–2450.

Goodwin B, Jones SA, Price RR, Watson MA, McKee DD, Moore LB, Galardi C, Wilson JG, Lewis MC, Roth ME, et al. (2000) A regulatory cascade of the nuclear receptors FXR, SHP-1, and LRH-1 represses bile acid biosynthesis. *Mol Cell* **6:**517–526.

Grober J, Zaghini I, Fujii H, Jones SA, Kliewer SA, Willson TM, Ono T, and Besnard P (1999) Identification of a bile acid-responsive element in the human ileal bile acid-binding protein gene. Involvement of the farnesoid X receptor/9-cis-retinoic acid receptor heterodimer. *J Biol Chem* **274:**29749–29754.

Huber RM, Murphy K, Miao B, Link JR, Cunningham MR, Rupar MJ, Gunyuzlu PL, Haws TF, Kassam A, Powell F, et al. (2002) Generation of multiple farnesoid-X-receptor isoforms through the use of alternative promoters. *Gene* **290:**35–43.

Kast HR, Goodwin B, Tarr PT, Jones SA, Anisfeld AM, Stoltz CM, Tontonoz P, Kliewer S, Willson TM, and Edwards PA (2002) Regulation of multidrug resistance-associated protein 2 (ABCC2) by the nuclear receptors pregnane X receptor, farnesoid X-activated receptor, and constitutive androstane receptor. *J Biol Chem* **277:**2908–2915.

Kim JB and Spiegelman BM (1996) ADD1/SREBP1 promotes adipocyte differentiation and gene expression linked to fatty acid metabolism. *Genes Dev* **10:**1096–1107.

Lambert G, Amar MJ, Guo G, Brewer HB Jr, Gonzalez FJ, and Sinal CJ (2003) The farnesoid X-receptor is an essential regulator of cholesterol homeostasis. *J Biol Chem* **278:**2563–2570.

Li J, Pircher PC, Schulman IG, and Westin SK (2005) Regulation of complement C3 expression by the bile acid receptor FXR. *J Biol Chem* **280:**7427–7434.

Lin FT and Lane MD (1994) CCAAT/enhancer-binding protein alpha is sufficient to initiate the 3T3–L1 adipocyte differentiation program. *Proc Natl Acad Sci USA* **91:**8757–8761.

Lu TT, Makishima M, Repa JJ, Schoonjans K, Kerr TA, Auwerx J, and Mangelsdorf DJ (2000) Molecular basis for feedback regulation of bile acid synthesis by nuclear receptors. *Mol Cell* **6:**507–515.

MacDougald OA and Mandrup S (2002) Adipogenesis: forces that tip the scales. *Trends Endocrinol Metab* **13:**5–11.

Pellicciari R, Fiorucci S, Camaioni E, Clerici C, Costantino G, Maloney PR, Morelli A, Parks DJ, and Willson TM (2002) 6alpha-ethyl-chenodeoxycholic acid (6-ECDCA), a potent and selective FXR agonist endowed with anticholestatic activity. *J Med Chem* **45:**3569–3572.

Rizzo G, Renga B, Antonelli E, Passeri D, Pellicciari R, and Fiorucci S (2005) The methyl transferase PRMT1 functions as co-activator of farnesoid x receptor (FXR)/9-cis retinoid X receptor and regulates transcription of FXR responsive genes. *Mol Pharmacol* **68:**551–558.

Rosen ED, Walkey CJ, Puigserver P, and Spiegelman BM (2000) Transcriptional regulation of adipogenesis. *Genes Dev* **14:**1293–1307.

Shishodia S and Aggarwal BB (2004) Guggulsterone inhibits NF-κB and IκBα kinase activation, suppresses expression of anti-apoptotic gene products, and enhances apoptosis. *J Biol Chem* **279:**47148–47158.

Sinal CJ, Tohkin M, Miyata M, Ward JM, Lambert G, and Gonzalez FJ (2000) Targeted disruption of the nuclear receptor FXR/BAR impairs bile acid and lipid homeostasis. *Cell* **102:**731–744.

Student AK, Hsu RY, and Lane MD (1980) Induction of fatty acid synthetase synthesis in differentiating 3T3–L1 preadipocytes. *J Biol Chem* **255:**4745–4750.

Tontonoz P, Hu E, and Spiegelman BM (1994) Stimulation of adipogenesis in fibroblasts by PPAR gamma 2, a lipid-activated transcription factor. *Cell* **79:**1147–1156.

Urizar NL, Dowhan DH, and Moore DD (2000) The farnesoid X-activated receptor mediates bile acid activation of phospholipid transfer protein gene expression. *J Biol Chem* **275:**39313–39317.

Urizar NL, Liverman AB, Dodds DT, Silva FV, Ordentlich P, Yan Y, Gonzalez FJ, Heyman RA, Mangelsdorf DJ, and Moore DD (2002) A natural product that lowers cholesterol as an antagonist ligand for FXR. *Science (Wash DC)* **296:**1703–1706.

Urizar NL and Moore DD (2003) GUGULIPID: a natural cholesterol-lowering agent. *Annu Rev Nutr* **23:**303–313.

Watanabe M, Houten SM, Wang L, Moschetta A, Mangelsdorf DJ, Heyman RA, Moore DD, and Auwerx J (2004) Bile acids lower triglyceride levels via a pathway involving FXR, SHP, and SREBP-1c. *J Clin Investig* **113:**1408–1418.

Wu Z, Rosen ED, Brun R, Hauser S, Adelmant G, Troy AE, McKeon C, Darlington GJ, and Spiegelman BM (1999) Cross-regulation of C/EBP alpha and PPAR gamma controls the transcriptional pathway of adipogenesis and insulin sensitivity. *Mol Cell* **3:**151–158.

Wu Z, Xie Y, Bucher NL, and Farmer SR (1995) Conditional ectopic expression of C/EBP beta in NIH-3T3 cells induces PPAR gamma and stimulates adipogenesis. *Genes Dev* **9:**2350–2363.

Xu H and Hotamisligil GS (2001) Signaling pathways utilized by tumor necrosis factor receptor 1 in adipocytes to suppress differentiation. *FEBS Lett* **506:**97–102.
Yamauchi T, Kamon J, Waki H, Imai Y, Shimozawa N, Hioki K, Uchida S, Ito Y, Takakuwa K, Matsui J, et al. (2003) Globular adiponectin protected ob/ob mice from diabetes and ApoE-deficient mice from atherosclerosis. *J Biol Chem* **278:** 2461–2468.
Zhang Y, Kast-Woelbern HR, and Edwards PA (2003) Natural structural variants of the nuclear receptor farnesoid X receptor affect transcriptional activation. *J Biol Chem* **278:**104–110.
Zhang Y, Ying Lee F, Barrera G, Lee H, Vales C, Gonzalez FJ, Willson TM, and Edwards PA (2006) Activation of the nuclear receptor FXR improves hyperglycemia and hyperlipidemia in diabetic mice. *Proc Natl Acad Sci USA* **103:**1006–1011.

Address correspondence to: Stefano Fiorucci, M.D., Dipartimento di Medicina Clinica e Sperimentale, University of Perugia, Via E dal Pozzo, 06122 Perugia, Italy. E-mail: fiorucci@unipg.it